IEEE Access
Multidisciplinary ⋮ Rapid Review ⋮ Open Access Journal

Received 28 July 2023, accepted 15 August 2023, date of publication 25 August 2023, date of current version 6 September 2023.

Digital Object Identifier 10.1109/ACCESS.2023.3308810

RESEARCH ARTICLE

Gender Differences in EEG Responses to Color and Black-White Images: Implications for Neuromarketing Strategies

ATEFE HASSANI[1], AMIN HEKMATMANESH[2], AND ALI MOTIE NASRABADI[1]
[1]Department of Biomedical Engineering, Shahed University, Tehran 3319118651, Iran
[2]Laboratory of Intelligent Machines, Lappeenranta University of Technology, 53850 Lappeenranta, Finland

Corresponding author: Amin Hekmatmanesh (amin.hekmatmanesh@lut.fi)

This work involved human subjects or animals in its research. Approval of all ethical and experimental procedures and protocols was granted by the National Ethics Committee in Biomedical Research.

ABSTRACT Analyzing the decision of different genders during shopping is an interesting topic in the neuromarketing industry. This study explores the EEG signal acquisition of twenty subjects in response to Color and Black-White (CL/BW) images and analysis both linear and nonlinear features in different brain regions. The Wilcoxon Rank Sum statistical test was utilized to determine the significance of features in identifying discriminative channels and frequency bands. The results show that the activation of different bands and regions are dependent on the subject's preference and the color of stimuli which are evaluated by spectral scalp map and power spectral density analysis on the the regions. Then, random forest, support vector machine, k-nearest neighbors, and linear discriminant analysis classifiers were also employed to identify the most significant active regions of different brain lobes in both human genders. For the female group in the Like task with CL/BW stimuli images, the classification accuracy significantly increased to 96.47% by combining all frequency bands in the random forest algorithm. On the other hand, for the male group, using the gamma frequency band in the k-nearest neighbors algorithm led to a notable improvement in classification accuracy, reaching 95.32% for the Like task with CL/BW stimuli images. The study provides insights into the influence of black-white colors on marketing products and neuromarketing strategies. The research also revealed differences in the time taken for males and females to make Like and Dislike decisions, as well as the decision-making time for Like and Dislike CL/BW images. The female group took approximately 2.5 seconds to choose an image of a product, whilst the male group took 2.5-3 seconds. The study's findings have significant implications for the field of neuromarketing, emphasizing the importance of careful stimulus selection and classifier choice for classification tasks.

INDEX TERMS EEG signal, classifier, decision making, gender, neuromarketing.

I. INTRODUCTION

Color is a highly effective marketing tool that significantly impacts an individual's psyche in advertising designs. It has the power to affect emotions, perceptions, performance, shopping behavior, and aggression, making it an essential element for the development of commercial products [1]. In fact, color plays a pivotal role in establishing the mood, emotions, and overall response when designing websites, business branding, and product selection. Studies have demonstrated that color is a critical product characteristic that is strongly linked to consumers' perception of a product [2]. Lai et al. [3], [4] have found that color has a more significant impact on product image than form and recommend providing consumers with a wide range of colors and product forms. Additionally, it has been reported that colors can attract attention and influence an individual's behavior [5].

Verbal feedback may not always provide an accurate reflection of an individual's response to color. In contrast,

The associate editor coordinating the review of this manuscript and approving it for publication was Larbi Boubchir.

physiological signals, such as the Electroencephalogram (EEG), can offer more reliable measurements. The EEG is a non-invasive method for recording the electrical activity of human brain, making it a relatively affordable and dependable tool with high temporal resolution and accuracy.

Numerous studies have investigated the impact of color on product selection. For instance, Arnab et al. [1] explored the cognitive effects of four color stimuli (red, green, yellow, and blue) and reported that red colors had the highest classification rate, while yellow colors had the lowest. Ma et al. [6] examined product customization using different color combinations and developed a decision-making support model to assist consumers in making effective purchase decisions and designing products. Additionally, Cimbalo et al. [7] analyzed the relationship between colors and emotions and reported that yellow, orange, and blue can evoke pleasant emotions. Furthermore, Kawasaki et al. [8] utilized EEG time series to investigate the effect of color preferences on neural mechanisms in the brain and found that theta power varied in the occipital region after selecting the preferred color.

Bagchi et al. [9] investigated the effect of a red background on the willingness to pay in auctions and reported a reduction in the offered price for the products. Similarly, Chen et al. [10] highlighted the importance of images and color in influencing investors' decisions about a product and found a negative effect of red color during decision making. Afterwards, Membreno et al. [11] examined the impact of color on the predisposition to purchase among social media users and suggested that the use of primary colors (red, yellow, and blue) in social network ads could influence consumers' willingness to purchase the advertised products. Furthermore, Rahmadani et al. [12] explored the impact of logo color on consumer memory and found that logo color changes could influence the active location of short-term memory.

In neuromarketing studies, power spectral density (PSD) is widely employed as a extracting features methods from EEG signals [13], [14]. Some studies propose that analyzing the PSD can help identify consumer preferences for products [15]. Additionally, frontal brain asymmetry features such as approach-withdrawal (AW) index, effort index, choice index, and valence are considered to be effective in determining consumer product preferences [16], [17], [18], [19]. Other common EEG features, such as differential entropy (DE) and Hjorth parameters, have been used in emotion recognition [20], [21]. Overall, there are limited studies on the utilization of these features and also liner and nonlinear features simultanously in neuromarketing.

Selecting appropriate EEG characteristics for the accurate prediction of product preferences (Likes or Dislikes) is a challenging task for neuromarketing researchers [22]. Consequently, it becomes important to conduct research that compares the classification accuracy of these features. This will facilitate future studies in the field of neuromarketing, enabling their application in a broader range of product like and dislike scenarios.

Building on the aforementioned concepts, our study aimed to investigate the impact of color on consumers' Like/Dislike decisions and willingness to purchase, by collecting EEG data from twenty participants using two different sets of stimuli, one comprising color stimuli and the other black-white stimuli with respect to the gender of participants. Our research contributed to three distinct areas: 1, identifying the most distinctive areas of brain associated with the Like/Dislike task, and 2, examining the EEG frequency bands in these identified regions, exploring both linear and nonlinear characteristics to differentiate between Like/Dislike conditions and CL/BW tasks when subjects liked or disliked the stimuli, with a focus on gender differences. Finally, our study used various features, such as PSD and energy of wavelet coefficients, fractal dimension, entropy, and trajectory volume behavior quantifiers, to train classifiers such as Random Forest, Support Vector Machine, K-Nearest Neighbors, and Linear Discriminative Analysis to interpret the Like/Dislike decisions in terms of subjects' willingness to pay for a product.

The paper is structured as follows. In Section II, we introduce the materials and methods used in our research. Section III presents the results of our statistical analysis and classifications. Finally, in Section IV, we provide concluding remarks.

II. MATERIALS AND METHODS

Here, The EEG data collected during the experiment were preprocessed using different methods and analyzed to investigate the neural activity associated with visual preference for shoes.

A. EXPERIMENTAL PARADIGM AND DATA RECORDING

A group of 20 healthy and voluntary right-handed university students (10 males and 10 females), aged between 22-30 years, participated in this study after providing a consent letter. The ethical approval for this study was obtained from the biomedical research committee with a registered code of IR.SHAHED.REC.1398.077The. Participants with a history of neurological or psychiatric disorders or those who consumed medication, alcohol, or drugs were excluded from the study. The EEG data were acquired while the participants were seated in a calm room and asked to maintain a steady posture in front of a screen placed at an appropriate distance. The participants were instructed to minimize blinking, eye movements, and any other body movements while keeping their eyes open and remaining calm. The stimulus images consisted of women's dress shoes displayed in various styles and colors.

Each participant in the experiment was asked to select their preferred image from a sequence of 16 color images and their corresponding black-white versions. The entire experiment lasted approximately 400 seconds for each participant. The whole experiment lasted about 400 seconds for each

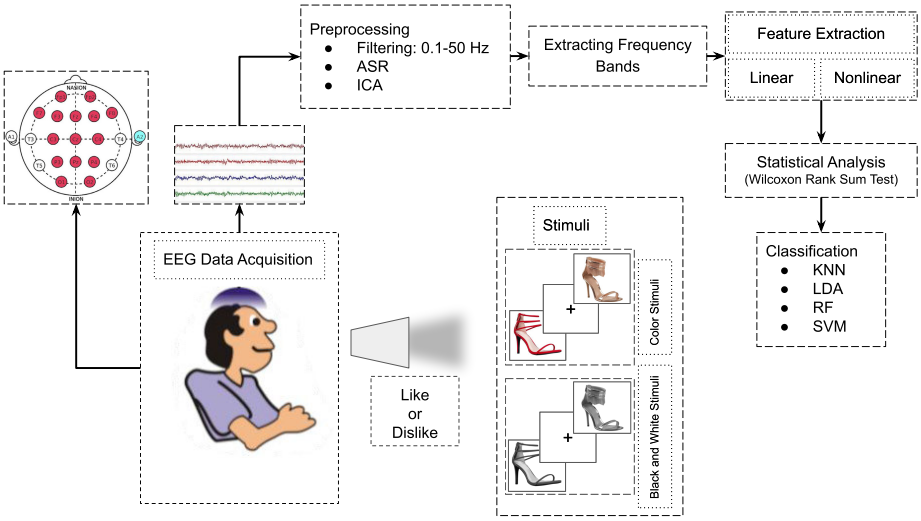

FIGURE 1. The study outline of analyzing data in the proposed system.

TABLE 1. Device and recording setting.

Setting	Value
Model	g.USBamp
Company	g.tec Austria
Channels	16
ADC	24bit
Sampling frequency	256 Hz
Reference	Fpz
GND	Right ear
Electrode placement	International 10-20 system

participant as they only had to click their preferred image from each choice for the full sequence of 16 color images, also the same images were rendered in black-white. We have used paradigm blocks for displaying images in the MATLAB software simulation environment.

For our experiment, we utilized a 16-channel EEG amplifier (g.USBamp, g.tec, Austria) with a sampling frequency of 256 Hz. The electrodes were positioned based on the international 10-20 electrode location system at Fp1, Fp2, F7, F3, Fz, F4, F8, C3, Cz, C4, P3, Pz, P4, O1, and O2. The GROUND (GND) electrode was placed on the right ear, while Fpz electrode was used as a common reference for all channels. The device and recording settings are presented in Table 1.

B. DATA ANALYSIS

Figure 1 depicts the data processing procedure. To minimize artifacts, an online high-pass filter and a notch filter with a cut-off frequency of 0.1 Hz and 50 Hz, respectively, were applied. The analytical procedures, which include Artifact Subspace Reconstruction (ASR) and Independent Component Analysis (ICA), are explained in detail below.

1) ARTIFACT SUBSPACE RECONSTRUCTION

Artifact Subspace Reconstruction (ASR) is a method used to automatically remove EEG artifacts by identifying and removing noisy components. This is achieved by decomposing EEG data into principal components (PCs) within time windows of the signal, and detecting components that exceed a predefined threshold [23], [24], [25]. The remaining PCs are then used to reconstruct the EEG data, resulting in a reduction of signal artifacts.

2) INDEPENDENT COMPONENT ANALYSIS (ICA)

Another method for reducing artifacts in EEG signals is by using, which is a component-based method used to separate linear sources. This method allows for the detection of different types of artifacts that have physiological and non-physiological sources, such as eye components, muscle components, heart components, line noise, channel noise, and others [26]. To provide a more accurate brain source diagnosis, we utilized the ICLable, ADJUST, and DIPFIT methods, which are available as plugins for the EEGLAB software within the MATLAB environment [27].

C. FEATURE EXTRACTION

The preprocessing of data is a crucial step in signal processing that can impact the performance of subsequent analyses. Several methodologies have been employed to identify the active regions of brain in response to marketing stimuli for different groups and to determine the most influential features and frequency bands in Like/Dislike and CL/BW analyses. To achieve these objectives, we analyzed the data using both linear and non-linear features, including entropy, fractal dimension, and volumetric behavior trajectory quantifiers [28], as detailed in Table 2.

Analyzing changes in features can help to characterize the effective brain regions in the Like/Dislike and CL/BW states. After applying the preprocessing algorithms mentioned in the previous section and retrieving the clean EEG signals, we decomposed the signal using the Discrete Wavelet Transform (DWT) with the Daubechies (db8) wavelet at

TABLE 2. Linear and non-linear features which are used in the study.

	Feature	Abbreviation	Description
Linear		PSD	Power spectral density
		EDWTC	Energy of discrete wavelet transform coefficients
Nonlinear	Entropy	SpE	Spectral entropy
		AE	Approximation entropy
		SE	Sample entropy
	Fractal Dimensions	HFD	Higuchi fractal dimensions
		KFD	Katz fractal dimensions
	volumetric behavior of signal's trajectory	OS	The average across all elements in matrix T
		AES	The average of negative numbers in matrix T''
		ACS	The average of positive numbers in matrix T''
		AE	The normalized expansion rate
		AC	The normalized compression rate
		SDES	Variation of negative numbers in matrix T''
		SDCS	Variation of positive numbers in matrix T''
		Complexity	Summation of the number of positive elements in SDCS (T'') and the number of negative elements in SDES (T'') after normalization

5 levels. The Wavelet Coefficient Energy (WCE) feature was extracted from the well-known EEG rhythms of delta, theta, alpha, beta, and gamma as follows:

$$E_i = \sum_{i=1}^{N} C_i, j^2 \tag{1}$$

In Eq. 1, where C_i, j represents the i-th coefficient of the j-band and N is the number of j-band coefficients.

To estimate the power spectral density (PSD) feature, we used a modified periodogram method that reduces the height of sidelobes or spectral leakage. The modified periodogram was computed for the five well-known frequency bands using a Hamming window.

The brain is a dynamic system that exhibits non-linear behavior. To gain insights into its complex nature, we can examine the properties of trajectories in phase space. By reconstructing a trajectory in phase space from time series data and extracting features or properties from it, we can track changes in the system. In our study, we utilized several entropy-based features that quantify the level of signal disorder and unpredictability of fluctuations in the time series data. Additionally, we used fractal-based features that measure the complexity of signal. These measures enable us to better understand the dynamics of brain.

In the final step, we extracted volumetric features which enable us to quantify the changes in the occupied space of trajectory. To achieve this, we reconstructed a phase space using two delayed EEG signals and computed the Euclidean distance matrices (T) of trajectories. Next, we obtained a modified matrix T' by excluding the main diagonal and removing the last column, which is then shifted to the left. The resulting matrix T'' represents the variation in the distances of state vectors and trajectory motion, from which the features were extracted.

Our study [29] presents a comprehensive understanding of the dynamic behavior of brain and sheds light on its complexity through the use of features described above. These features have been utilized to achieve our objective.

D. STATISTICAL ANALYSIS

Non-parametric methods are a class of statistical procedures that require minimal assumptions about the underlying data distribution and facilitate obtaining approximate and exact P-values for statistical tests [30]. One such method is the Wilcoxon Rank Sum test, which tests the hypothesis that two independent samples are drawn from populations with equal medians.

In our study, after extracting the features, we employed the Wilcoxon Rank Sum test to identify distinctive channels in each frequency band. The discrimination criterion between the Like/Dislike and CL/BW groups was a significant level of 1%.

E. CLASSIFICATION

In this study, we employed Random Forest, Support Vector Machine, K-Nearest Neighbors, and Linear Discriminant Analysis classifiers, which are elaborated below, to pinpoint the crucial activation regions of various brain lobes in both male and female genders.

1) RANDOM FOREST (RF)

RF is a widely used supervised learning algorithm in machine learning. It constructs multiple decision trees using different samples from the data and takes a majority vote for classification or an average for regression. The key advantages of RF Algorithm is its ability to handle datasets containing both categorical and continuous variables for both classification and regression problems. Additionally, the algorithm is less prone to overfitting and typically produces better results compared to other classification approaches.

2) SUPPORT VECTOR MACHINE (SVM)

SVM is a popular supervised machine learning algorithm used for classification and regression tasks. The SVM classifier builds a model that separates data points into different categories using a hyperplane. In this study, the Radial Basis Function (RBF) kernel was used as a measure of similarity between data points, allowing for non-linear classification [31].

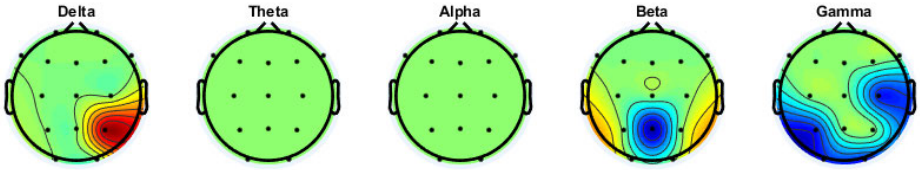

(a) Displaying Linear Features Through Brain Mapping for Female Subjects

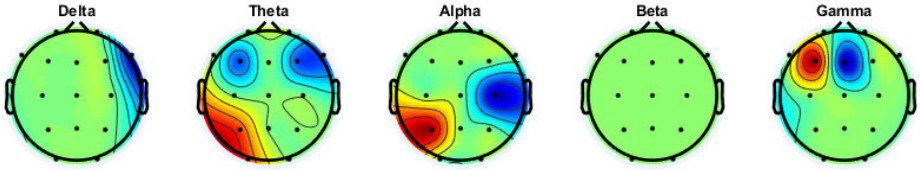

(b) Displaying Nonlinear Features Through Brain Mapping for Female Subjects

FIGURE 2. The identified distinct brain regions in female subjects participated in a Like/Dislike task involving the presentation of black-white images. (a) Linear and (b) nonlinear features were employed to identify distinct brain regions.

3) K-NEAREST NEIGHBORS (KNN)

KNN algorithm is a simple, non-parametric, and supervised machine learning algorithm that can be used for regression or classification problems. Unlike model-based methods, KNN does not have a training stage. Classification tasks are performed by calculating the distance between the test sample and all training samples and then classifying the sample based on the K-nearest neighbors. KNN is popular due to its simplicity and significant classification performance [32], [33], [34], [35], [36], [37].

4) LINEAR DISCRIMINANT ANALYSIS (LDA)

LDA is a statistical method developed by R. Fisher. Originally used for classifying different types of flowers, it has since become a popular technique for both classification and dimension reduction applications.

The assessment of classifiers' efficacy utilizing EEG signals from different brain lobes (frontal, central, parietal, and occipital) was conducted using three performance metrics including accuracy, sensitivity, and specificity. These three terms were calculated from the confusion matrix, which is a 2×2 matrix with the following fields: true positive (TP), true negative (TN), false positive (FP), and false negative (FN). The following matrix illustrates the fields of a typical confusion matrix, which can be formulated as follows [38]:

$$\begin{aligned} Accuracy &= (TP + TN)/(TP + TN + FP + FN) \\ Sensiivity &= TP/(TP + FN) \\ Specificity &= TN/(FP + TN) \end{aligned}$$

III. EXPERIMENTAL RESULTS AND DISCUSSION

In the experiment, EEG signals were recorded from twenty subjects and they were presented with both CL/BW images. In the preprocessing step, we removed various types of artifacts from the total Like and Dislike epochs, each of which was 15 seconds long. The experimental results comprise the analysis of frequency bands, brain regions, and the impact of nonlinear and linear features on the identified brain regions. The identified brain regions were extracted using the Wilcoxon Rank Sum statistical test. The Wilcoxon Rank Sum statistical test was utilized to determine the significance of features in identifying discriminative channels. The impact of BW images in a Like/Dislike task was explored. Furthermore, the study investigated the effects of CL/BW images on brain activity when subjects expressed their liking or disliking of the images.

A. STATISTICAL ANALYSIS OF LINEAR FEATURES VS. NON-LINEAR FEATURES

The results are presented in the form of color-coded brain maps where the red regions indicate channels where the average extracted features for the Like condition are greater than those for the Dislike condition. Conversely, the blue regions denote channels where the average extracted features for the Dislike condition are greater than those for the Like condition.

1) ANALYSIS ON THE IMPACT OF BLACK-WHITE IMAGES IN A LIKE/DISLIKE TASK

In this section, we investigate and extract the distinct brain regions of participants with respect to their genders in a Like/Dislike task using BW images as stimuli.

a: ANALYSIS OF FEMALE SUBJECTS RESULTS

Figure 2 displays the scalp maps of the average extracted linear/nonlinear features for discriminative channels and frequency bands between the Like and Dislike conditions of female subjects while displaying BW images.

A) Results using linear features are shown in Figure 2a. The delta band in the right parietal channel was found to be the most effective and activated region for the Like condition. The Dislike condition showed the following most effective and activated regions: beta band in the middle parietal (Pz)

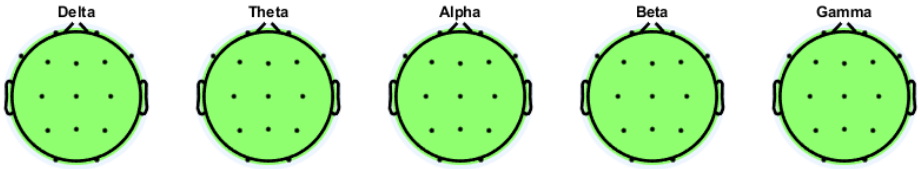

(a) Displaying Linear Features Through Brain Mapping for male Subjects

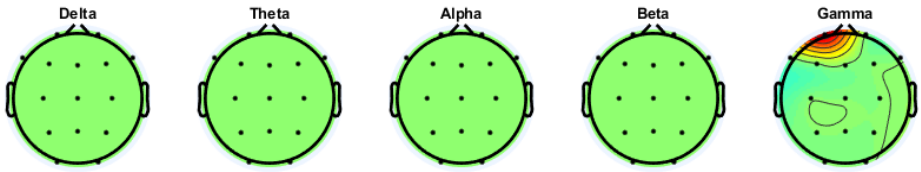

(b) Displaying Nonlinear Features Through Brain Mapping for male Subjects

FIGURE 3. The identified distinct brain regions in male subjects participated in a Like/Dislike task involving the presentation of black-white images. (a) Linear and (b) nonlinear features were employed to identify distinct brain regions.

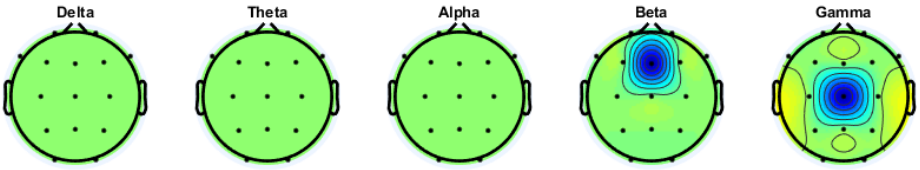

(a) Displaying Linear Features Through Brain Mapping for Combination of Male and Female Subjects

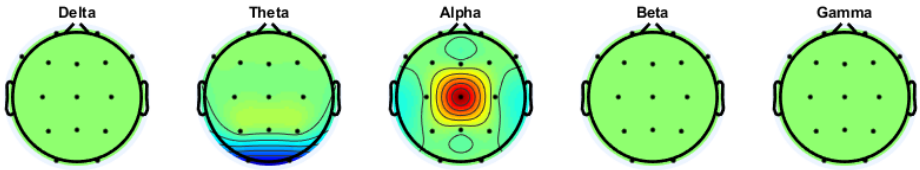

(b) Displaying Nonlinear Features Through Brain Mapping for the Combination of Male and Female Subjects

FIGURE 4. The identified distinct brain regions in the combination of male and female subjects participated in a Like/Dislike task involving the presentation of black-white images. (a) Linear and (b) nonlinear features were employed to identify distinct brain regions.

and gamma band in the occipital (O1, O2), left parietal (P3), and right central (C4) regions. There were no significant changes observed in the theta and alpha bands. B) Results using nonlinear features are shown in Figure 2b. The theta band in the left parietal and occipital regions (P3 and O1), the alpha band in the left parietal (P3), and the gamma band in the left frontal (F3) regions were found to be the most effective and activated regions for the Like condition. Additionally, the Dislike condition showed dominance in the right frontal (F8) region for the delta band, right and left frontal (F3, F4, and F8) regions for the theta band, the right central (C4) region for the alpha band, and the middle frontal (Fz) region for the gamma band. There were no significant changes observed in the beta band.

b: ANALYSIS OF MALE SUBJECTS RESULTS

Figure 3 displays the scalp maps of male subjects showing the average extracted linear/nonlinear features for discriminative channels and frequency bands between the two groups Like/Dislike during displaying black-white images.

A) Using the linear features, as shown in Figure 3a, no significant changes or effective channels were identified for the Like and Dislike conditions across the five different frequency bands. B) On the other hand, using nonlinear features, Figure 3b illustrates that the gamma frequency band in the left frontal (Fp1) region was the most effective and activated region for the Like condition. The results showed insignificant changes in the delta, theta, alpha, and beta bands for both Like and Dislike conditions.

c: ANALYSIS OF COMBINED MALE AND FEMALE SUBJECTS RESULTS

Figure 4 displays the scalp maps of all subjects (males and females) depicting the average extracted linear/nonlinear features obtained for discriminative channels and frequency bands between the Like/Dislike groups while displaying black-white images.

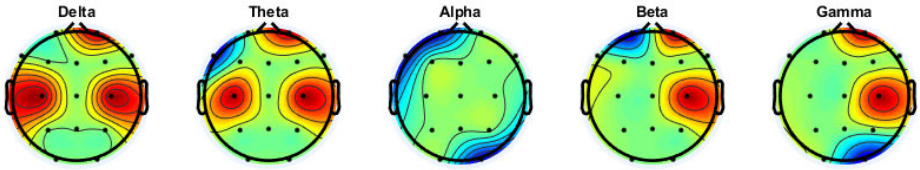

(a) Visualization of Linear Features in Brain Mapping of Female Participants in Response to Liked Stimulus Images.

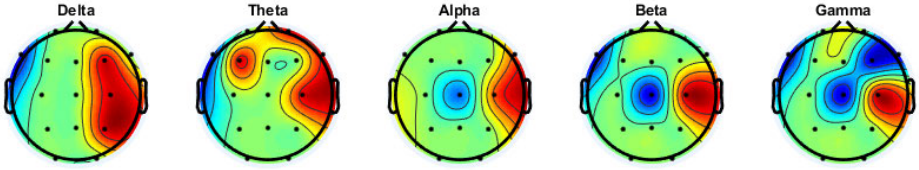

(b) Visualization of Linear Features in Brain Mapping of Female Participants in Response to Disliked Stimulus Images.

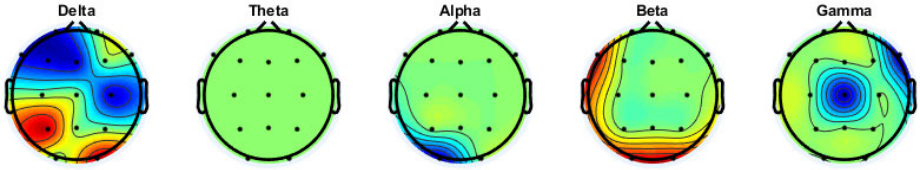

(c) Visualization of Nonlinear Features in Brain Mapping of Female Participants in Response to Liked Stimulus Images.

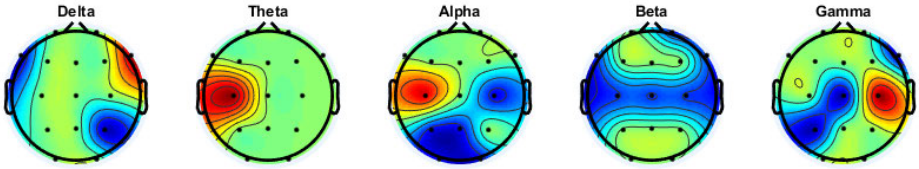

(d) Visualization of Nonlinear Features in Brain Mapping of Female Participants in Response to Disliked Stimulus Images.

FIGURE 5. Visualization of the obtained linear and nonlinear features in distinct brain regions of female participants in response to liked and disliked stimuli CL/BW images.

A) Utilizing linear features, Figure 4a reveals that the beta band in the middle frontal (Fpz) channel and the gamma band in the middle central (Cz) region are the most effective and activated regions for the Dislike condition. No significant changes in the five frequency bands were observed for the Like condition. B) Utilizing nonlinear features, as depicted in Figure 4b, the most effective and activated region for the Like condition is the alpha band in the middle central (Cz) region. Furthermore, the Dislike condition exhibited dominance in the right and left occipital (O1, O2) regions for the theta band. No significant changes in the delta, beta, and gamma bands were observed for either Like or Dislike conditions.

2) ANALYSIS ON THE IMPACT OF CL/BW IMAGES IN LIKE/DISLIKE TASKS

Our study examined the impact of color versus BW images on subjective preferences in various participant groups, utilizing both linear and nonlinear features. We hypothesized that red regions would indicate channels in which average extracted features for color images are greater than those for black-white images in both Like and Dislike situations, while blue regions would denote channels where the opposite is true.

a: FEMALES BRAIN MAP ANALYSIS

Figure. 5 illustrates the distinct brain regions of female subjects that were identified while viewing CL/BW images, utilizing both linear and nonlinear features to assess subjective Likes and Dislikes.

A) Utilizing Linear Features, Figure 5a illustrates the distinct brain regions identified when participants liked the CL/BW stimuli. Discriminative channels for the color task were observed in the delta and theta bands of central (C3 and C4) regions and right frontal (Fp2) region, as well as the beta and gamma bands in the right central (C4) and right

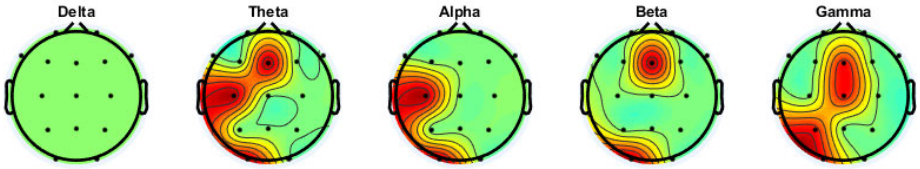

(a) Visualization of Linear Features in Brain Mapping of Male Participants in Response to Liked Stimulus Images.

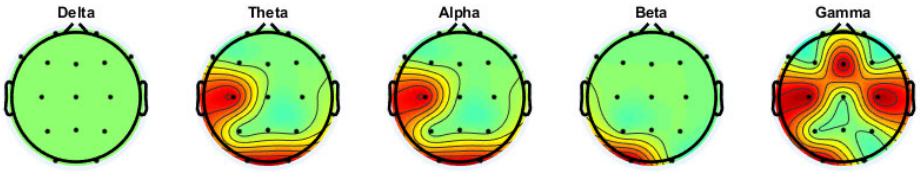

(b) Visualization of Linear Features in Brain Mapping of Male Participants in Response to Disliked Stimulus Images.

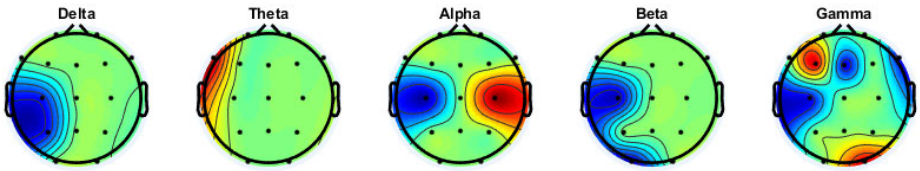

(c) Visualization of Nonlinear Features in Brain Mapping of Male Participants in Response to Liked Stimulus Images.

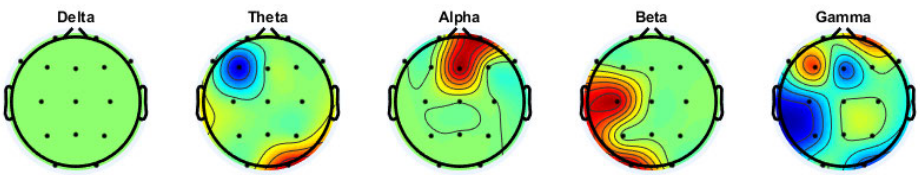

(d) Visualization of Nonlinear Features in Brain Mapping of Male Participants in Response to Disliked Stimulus.

FIGURE 6. Visualization of the obtained linear and nonlinear features in distinct brain regions of male participants in response to liked and disliked stimuli CL/BW images.

frontal (Fp2)regions. Insignificant changes were observed in the alpha band. The distinct and effective channels for the black-white task were observed in the left frontal region in the theta, the alpha band in the left frontal (F7, Fp1) regions and right occipital (O2) region, the beta band in the left prefrontal (Fp1) region, the gamma band in the right occipital (O2) region and insignificant changes were observed in the delta band. Referring to Figure 5b, the delta band in the right frontal, central, and parietal (F4, C4, P4) regions, the theta band in the left frontal (F3), right frontal (F8, Fp2), and right central (C4) regions, the alpha band in the right central (C4) and right frontal (F8) regions, and the beta and gamma bands in the right central (C4) regions were the most distinct channels observed in the color task when subjects expressed Dislike toward the stimuli. Similarly, the delta and theta bands in the left frontal (F7) region, the alpha band in the middle central (Cz) region, the beta band in the middle central (Cz) and left frontal (F7) regions and the gamma band in the middle central (Cz), frontal (F7, F4, and F8) regions were the most discriminative channels for the black-white task when subjects expressed Dislike toward the stimuli.

B) Using the non-linear features, the results for both the Like and Dislike conditions are summarized in Figure 5c and Figure 5d. As depicted in Figure 5c, the most effective regions for the color task when subjects expressed liking toward the stimuli were the delta band in the left parietal (P3) and right occipital (O2) regions, as well as the beta band in the left frontal (F7) and occipital (O1 and O2) regions, while there were insignificant changes observed for the theta, alpha, and gamma frequency bands. In addition, the delta band in the right central (C4), left frontal (Fp1, F3, and F7) regions, the alpha band in the left occipital (O1) region, and the gamma band in the middle central (Cz) and right frontal (F8) regions were significantly discriminative channels for the black-white task. However, there were insignificant changes observed for the theta and beta frequency bands. Figure 5d

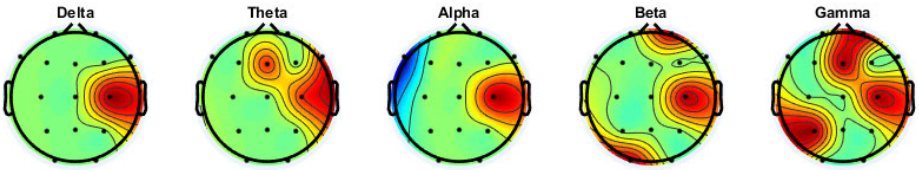

(a) Visualization of Linear Features in Brain Mapping of Combined Male and Female Participants in Response to Liked Stimulus.

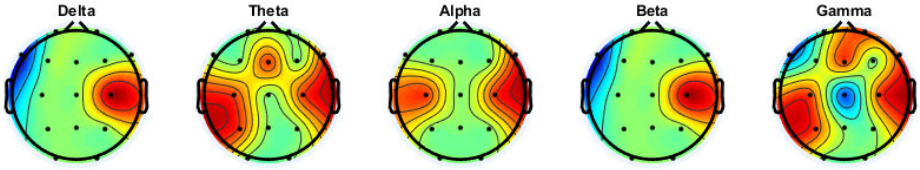

(b) Visualization of Linear Features in Brain Mapping of Combined Male and Female Participants in Response to Disliked Stimulus.

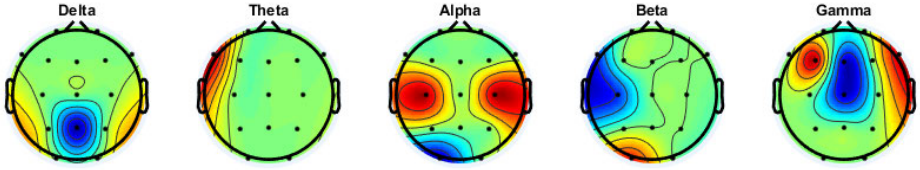

(c) Visualization of Nonlinear Features in Brain Mapping of Combined Male and Female Participants in Response to Liked Stimulus.

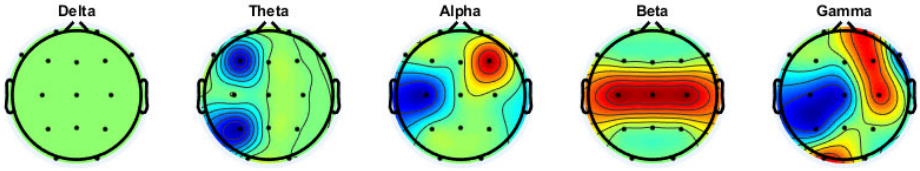

(d) Visualization of Nonlinear Features in Brain Mapping of Combined Male and Female Participants in Response to Disliked Stimulus.

FIGURE 7. Visualization of the obtained linear and nonlinear features in distinct brain regions of combined genders participants in response to liked and disliked stimuli CL/BW images.

illustrates the effective channels in different frequency bands during the color and BW tasks, in response to stimuli that participants disliked. For the color task, the effective channels were identified as the delta band in the right frontal (F8) region and the theta and alpha bands in the left central (C3) regions. The right central (C4) region showed a significant response in the gamma band. However, there was no significant change observed in the beta frequency band. Similarly, for the BW task, the effective channels were identified as the delta band in the left frontal (F7) and right parietal (P4) regions. The alpha band showed significant activity in the right central (C4), left and middle parietal (P3, Pz), and occipital (O1, O2) regions, while the beta band showed activity in the central (C3, Cz, and C4) and frontal (Fp2, F8, and F7) regions. The right frontal (F8), middle central (Cz), and left parietal (P3) regions showed significant activity in the gamma band. However, no significant change was observed in the theta frequency band.

b: MALES BRAIN MAP ANALYSIS

Figure 6 displays the discriminative brain regions identified in male subjects in response to displaying CL/BW images using both linear and non-linear features, and whether the stimuli were liked or disliked.

A) Results using linear features: Figure 6a displays the most discriminative brain regions observed in male participants when they liked the CL/BW stimuli, using linear features. For the color task, the middle frontal region, and the left central (C3) and occipital (O1) channels in the theta band, as well as the central and occipital channels on the left (C3, O1) in the alpha band, a frontal channel on the middle (Fz) and occipital on the left (O1) in the beta band, and frontal (Fz), central (Cz) channels, parietal and occipital on the left (P3, O1) in the gamma band, were identified as the most discriminative channels. On the other hand, when male subjects disliked the stimulus images, Figure 6b shows that the most distinct channels were the left central (C3) and occipital (O1, O2) channels in the theta and alpha bands, the

left occipital (O1) channel in the beta band, the middle frontal (Fz), central (C3, C4), and the left occipital (O1) channels in the gamma band. No significant change was observed in the five frequency bands for the BW task, in both the Like and Dislike conditions.

B) Utilizing Non-linear Features: Figure 6c and Figure 6d summarize the results for both Like and Dislike conditions. Figure 6c illustrates the most discriminative brain regions in male participants who liked the CL/BW stimuli. For the color task, the distinct channels were located on the left frontal (F7) in the theta band, right central (C4) in the alpha band, and left frontal (F3) and right occipital (O2) regions in the gamma band. Furthermore, for the BW task, the distinct channels were located on the left central (C3) and parietal (P3) in the delta band, left central in the alpha band, central and occipital channels on the left (C3, O1) in the beta band, and left central (C3) and frontal (Fz, F8) channels in the gamma band. The most discriminative channels for male participants who disliked the CL/BW stimuli are shown in Figure 6d. For the color task, the obtained regions are as follows: right occipital channel (O2) in the theta band, frontal channels (Fz, Fp2) in the alpha band, central and occipital channels on the left (C3, O1) in the beta band, and frontal channels (F3, Fp2) in the gamma band. On the other hand, for the BW task, the most impactful channels are as follows: frontal channels on the left (F3) in the theta band, left central (C3), left parietal (P3), middle frontal (Fz), and right occipital (O2) in the gamma band.

c: ANALYSIS ON THE BRAIN MAP OF COMBINED MALE AND FEMALES

Figure 7 displays the discriminative brain regions identified in both male and female participants while viewing CL/BW images, using linear and non-linear features to study their response to stimuli they liked or disliked.

When linear features were used, Figure 7a illustrates the effective channels in different frequency bands for participants who liked the CL/BW stimuli. In the color task, the channels were located in the delta and alpha bands in the right central (C4) region, the theta band in frontal (Fz, F8) and right central (C4) regions, the beta band in the right central (C4), right prefrontal (Fp2), and left occipital (O1) regions, and the gamma band in frontal (Fp1, Fz), right central, and left parietal (P3) regions. Additionally, the channel for the BW task was the alpha band in the left frontal (F7) region, with no significant change in the delta, theta, beta, and gamma frequency bands. In Figure 7b, the most discriminative channels for the color task when participants disliked the stimuli were identified in the delta and beta bands in the right central (C4) region, the theta band in frontal (Fz, F8), central (C3, C4), and left parietal (P3) regions, the alpha band in central (C3, C4), and right frontal (F8) regions, and the gamma bands in frontal (Fp2, Fz, F8), central (C3, C4), and left parietal (P3) regions. Moreover, the delta and beta bands in the left frontal (F7) region and the gamma band in the left frontal (F7) and middle central (Cz) regions were the most discriminative channels for the BW task when participants disliked the stimuli.

B) Non-linear features were also used to derive results for both Like and Dislike conditions, as shown in Figures 7c and 7d. Figure 7c indicates that the most discriminative brain regions for all participants when they liked the CL/BW stimuli. For the color task, distinct channels were observed in the left frontal (F7) region in the theta band, central regions (C3, C4) in the alpha band, left occipital (O1) region in the beta band, and left and right frontal regions (F3, F8) in the gamma band. For the BW task, the middle parietal region (Pz) in the delta band, left occipital region (O1) in the alpha band, left central and frontal regions (C3, F7) in the beta band, and middle frontal and central regions (Fz, Cz) in the gamma band were the most discriminative channels. Regarding the male participants who disliked the CL/BW stimuli, Figure 7d shows the most discriminative channels. For the color task, the regions that were most affected include the right frontal channel (F4) in the alpha band, central channels (C3, Cz, C4) in the beta band, and right frontal (F4, Fp2), right central (C4), and left occipital (O1) channels. For the BW task, the most impactful channels were observed in the left frontal (F3) and left parietal (P3) regions in the theta band, central regions on the left (C3) in the alpha band, and left central, middle central (Cz) and parietal (P3) regions in the gamma band.

B. CLASSIFICATION RESULTS

In this section, we investigate the performance of different classifiers and identify the activation regions of various brain lobes in response to black-white stimuli. This analysis sheds light on the impact of CL/BW stimuli on both marketing products and neuromarketing strategies.

Firstly, linear and non-linear features were computed for different groups of participants in the given frequency bands. Then, the Wilcoxon Rank Sum test was performed to determine the significance of features. The p-values for each test were set at 0.01, and values less than this level were considered significant and preserved for the classification task. These significant values were fed into four conventional classification algorithms, namely KNN, LDA, RF, and SVM.

The performance of each classifier based on EEG signals from the frontal, central, parietal, and occipital brain lobes was evaluated in terms of three metrics, namely classification accuracy, sensitivity, and specificity.

1) PERFORMANCE ANALYSIS OF LIKE/DISLIKE TASKS FOR BW STIMULI

The results presented in Table 3 indicate that the combination of delta, beta, and gamma bands using linear features achieved the highest accuracy for female subjects, with the energy of discrete wavelet transform coefficient feature being the most informative. The SVM classifier outperformed other classifiers, including KNN, LDA, and RF, achieving a classification accuracy of 69.12%. In contrast, for male subjects, the gamma band using non-linear features with the KNN classifier achieved the best accuracy of 64.25%,

TABLE 3. Classification results for like/dislike task using linear and nonlinear features with black-white images, across different groups.

Group	Features	Classifier	Metric	Delta	Theta	Alpha	Beta	Gamma	All Bands
Females	Linear	KNN	Accuracy	62.90 ± 4.40	-	-	50.84 ± 7.16	64.06 ± 9.64	59.42 ± 5.11
			Sensitivity	60.21 ± 4.85	-	-	46.84 ± 12.82	61.43 ± 10.78	71.24 ± 13.20
			Specificity	65.49 ± 5.92	-	-	54.83 ± 4.83	66.72 ± 10.58	47.94 ± 9.04
		LDA	Accuracy	63.11 ± 5.19	-	-	63.32 ± 6.19	65.51 ± 2.93	62.08 ± 4.29
			Sensitivity	68.17 ± 7.90	-	-	65.06 ± 7.51	59.69 ± 2.10	66.57 ± 7.12
			Specificity	58.22 ± 3.52	-	-	61.62 ± 6.18	71.26 ± 5.04	57.75 ± 3.17
		RF	Accuracy	60.62 ± 11.04	-	-	47.5 ± 11.48	60.00 ± 10.29	61.25 ± 13.44
			Sensitivity	55.95 ± 21.93	-	-	45.02 ± 24.54	60.63 ± 8.03	62.97 ± 16.37
			Specificity	64.22 ± 18.45	-	-	49.16 ± 16.10	59.32 ± 18.48	59.78 ± 18.41
		SVM	Accuracy	63.21 ± 2.36	-	-	64.15 ± 3.88	66.50 ± 6.30	69.12 ± 3.88 ↑
			Sensitivity	57.59 ± 4.28	-	-	51.29 ± 3.93	80.28 ± 5.32	72.54 ± 5.43
			Specificity	68.71 ± 3.97	-	-	76.36 ± 8.84	53.64 ± 8.34	65.65 ± 4.68
	Nonlinear	KNN	Accuracy	58.44 ± 4.18	58.97 ± 6.51	58.17 ± 5.24	-	51.67 ± 2.19	64.27 ± 2.35
			Sensitivity	64.25 ± 10.00	61.03 ± 6.06	53.42 ± 4.64	-	50.20 ± 3.04	54.98 ± 7.68
			Specificity	52.79 ± 7.28	56.93 ± 7.40	62.81 ± 6.09	-	53.08 ± 5.91	73.32 ± 7.96
		LDA	Accuracy	63.75 ± 2.80	56.62 ± 2.84	61.38 ± 3.53	-	60.58 ± 1.92	58.62 ± 3.05
			Sensitivity	62.44 ± 7.90	57.89 ± 7.09	50.93 ± 5.17	-	58.26 ± 4.95	52.55 ± 3.33
			Specificity	63.06 ± 7.11	55.55 ± 4.28	71.96 ± 4.17	-	63.01 ± 8.72	64.75 ± 7.33
		RF	Accuracy	58.12 ± 8.86	65.62 ± 12.93	57.50 ± 11.33	-	54.37 ± 11.43	67.50 ± 8.23
			Sensitivity	62.87 ± 20.72	62.29 ± 20.67	58.26 ± 18.83	-	48.31 ± 13.47	66.07 ± 18.83
			Specificity	60.01 ± 19.89	69.76 ± 19.84	58.99 ± 16.57	-	58.56 ± 20.97	69.69 ± 13.45
		SVM	Accuracy	62.81 ± 4.77	63.14 ± 2.81	64.24 ± 4.41	-	66.20 ± 5.31	68.52 ± 6.70 ↑
			Sensitivity	50.85 ± 6.79	47.03 ± 4.34	60.47 ± 3.61	-	56.51 ± 7.64	72.06 ± 10.94
			Specificity	75.09 ± 4.40	79.02 ± 2.66	68.11 ± 7.43	-	75.92 ± 5.92	65.22 ± 4.79
Males	Nonlinear	KNN	Accuracy	-	-	-	-	64.25 ± 9.80 ↑	54.80 ± 3.06
			Sensitivity	-	-	-	-	63.20 ± 8.88	54.22 ± 1.76
			Specificity	-	-	-	-	65.33 ± 11.92	55.38 ± 4.89
		LDA	Accuracy	-	-	-	-	60.97 ± 3.92	56.42 ± 2.31
			Sensitivity	-	-	-	-	35.43 ± 4.30	38.81 ± 2.74
			Specificity	-	-	-	-	85.81 ± 8.94	74.70 ± 2.98
		RF	Accuracy	-	-	-	-	56.67 ± 12.27	56.00 ± 8.43
			Sensitivity	-	-	-	-	46.46 ± 13.94	60.04 ± 16.27
			Specificity	-	-	-	-	69.94 ± 15.88	53.25 ± 19.12
		SVM	Accuracy	-	-	-	-	56.39 ± 3.78	57.19 ± 2.74
			Sensitivity	-	-	-	-	47.06 ± 7.96	56.30 ± 6.40
			Specificity	-	-	-	-	65.13 ± 1.77	58.07 ± 2.15
All Subjects	Linear	KNN	Accuracy	-	-	-	63.90 ± 4.36 ↑	53.89 ± 3.07	54.39 ± 2.87
			Sensitivity	-	-	-	65.45 ± 5.13	53.60 ± 2.99	60.57 ± 1.63
			Specificity	-	-	-	62.34 ± 3.88	54.18 ± 4.38	48.22 ± 5.79
		LDA	Accuracy	-	-	-	61.02 ± 2.92	55.07 ± 1.66	61.18 ± 2.94
			Sensitivity	-	-	-	55.10 ± 2.28	36.48 ± 2.46	54.04 ± 3.15
			Specificity	-	-	-	66.89 ± 6.07	73.73 ± 3.00	65.28 ± 7.72
		RF	Accuracy	-	-	-	58.33 ± 6.71	56.00 ± 7.82	52.33 ± 9.34
			Sensitivity	-	-	-	61.25 ± 8.02	51.72 ± 10.12	54.64 ± 16.43
			Specificity	-	-	-	53.89 ± 16.7	61.61 ± 12.83	50.41 ± 14.63
		SVM	Accuracy	-	-	-	61.23 ± 2.64	60.12 ± 2.51	59.71 ± 4.61
			Sensitivity	-	-	-	54.68 ± 3.79	68.75 ± 3.76	60.94 ± 7.49
			Specificity	-	-	-	67.81 ± 2.08	51.50 ± 4.46	58.48 ± 5.02
	Nonlinear	KNN	Accuracy	-	51.10 ± 4.43	55.00 ± 3.86	-	-	56.39 ± 4.60
			Sensitivity	-	49.52 ± 4.05	56.12 ± 4.78	-	-	58.43 ± 5.71
			Specificity	-	52.71 ± 5.01	53.87 ± 3.67	-	-	54.38 ± 4.37
		LDA	Accuracy	-	58.14 ± 2.36	61.66 ± 2.55	-	-	65.03 ± 2.48 ↑
			Sensitivity	-	65.49 ± 3.28	47.21 ± 1.90	-	-	62.80 ± 4.90
			Specificity	-	50.77 ± 3.28	76.12 ± 4.32	-	-	67.27 ± 0.72
		RF	Accuracy	-	50.00 ± 5.66	54.33 ± 7.38	-	-	59.67 ± 8.08
			Sensitivity	-	45.44 ± 9.87	56.99 ± 12.74	-	-	60.02 ± 12.65
			Specificity	-	56.14 ± 13.98	50.68 ± 9.32	-	-	58.18 ± 14.93
		SVM	Accuracy	-	54.51 ± 2.01	60.69 ± 1.33	-	-	62.10 ± 2.68
			Sensitivity	-	53.89 ± 5.50	53.47 ± 2.77	-	-	64.79 ± 1.68
			Specificity	-	55.13 ± 9.02	67.87 ± 2.07	-	-	59.42 ± 5.09

with the SDES and complexity features providing the most informative data. Linear features did not show any significant differences in features compared to non-linear features. Moreover, the combination of theta and alpha frequency bands using non-linear features achieved the highest accuracy of 65.03% for both female and male subjects. The LDA classifier outperformed other classifiers, including KNN, RF, and SVM, in this study. The algorithm identified sample and spectral entropy as the most informative features among those that were extracted.

2) PERFORMANCE ANALYSIS OF LIKE AND DISLIKE TASKS FOR CL/BW STIMULI

The results presented in Table 4 demonstrate that the combination of delta, theta, alpha, beta, and gamma frequency bands produced the most accurate feature set for classifying female subjects when they liked CL/BW stimuli, with a classification accuracy of 96.47%. This combination using linear features outperformed other feature sets, including nonlinear features. Furthermore, the RF classifier exhibited better performance than other classifiers such as KNN,

TABLE 4. Classification results for like task using linear and nonlinear features with CL/BW stimuli images, across different groups.

Group	Features	Classifier	Metric	Delta	Theta	Alpha	Beta	Gamma	All Bands
Females	Linear	KNN	Accuracy	85.16 ± 3.06	92.71 ± 2.70	74.01 ± 3.49	82.51 ± 3.69	93.82 ± 3.22	95.24 ± 1.06
			Sensitivity	85.51 ± 3.39	95.65 ± 1.89	72.01 ± 3.93	81.50 ± 4.71	92.52 ± 3.69	93.29 ± 2.31
			Specificity	84.80 ± 4.08	89.75 ± 4.10	76.03 ± 9.03	83.54 ± 3.03	9.15 ± 3.70	97.08 ± 2.33
		LDA	Accuracy	68.81 ± 4.02	66.19 ± 6.43	64.07 ± 7.97	67.37 ± 5.71	69.05 ± 5.76	78.65 ± 3.90
			Sensitivity	78.20 ± 6.11	66.23 ± 6.94	58.28 ± 7.13	69.51 ± 7.86	75.44 ± 5.32	72.98 ± 6.07
			Specificity	59.55 ± 6.51	66.18 ± 7.49	69.63 ± 9.65	65.13 ± 3.10	62.67 ± 6.59	84.27 ± 4.89
		RF	Accuracy	81.18 ± 9.11	87.65 ± 7.04	67.06 ± 8.86	82.35 ± 9.60	89.41 ± 8.68	96.47 ± 4.11 ↑
			Sensitivity	82.92 ± 15.40	87.66 ± 12.71	67.40 ± 14.87	80.55 ± 14.94	88.49 ± 6.77	93.28 ± 9.85
			Specificity	80.36 ± 10.61	89.03 ± 9.88	67.06 ± 9.10	84.11 ± 12.24	89.44 ± 13.10	98.75 ± 3.95
		SVM	Accuracy	65.50 ± 3.68	72.31 ± 5.03	67.09 ± 3.29	71.19 ± 3.50	82.36 ± 3.41	92.51 ± 1.60
			Sensitivity	72.36 ± 7.42	71.68 ± 3.05	80.90 ± 3.19	63.31 ± 5.63	75.90 ± 1.38	90.72 ± 3.13
			Specificity	58.90 ± 2.69	72.95 ± 7.31	53.34 ± 4.84	78.81 ± 1.94	88.73 ± 6.60	94.29 ± 3.45
	Nonlinear	KNN	Accuracy	66.99 ± 2.18	-	55.60 ± 2.10	65.29 ± 3.95	62.72 ± 3.45	72.59 ± 3.49
			Sensitivity	71.30 ± 3.69	-	60.12 ± 4.34	69.79 ± 8.48	59.65 ± 4.00	78.82 ± 4.24
			Specificity	62.82 ± 2.22	-	51.03 ± 2.91	60.79 ± 3.45	65.51 ± 6.62	66.32 ± 3.57
		LDA	Accuracy	71.03 ± 4.91	-	62.27 ± 2.96	61.12 ± 1.94	69.38 ± 3.10	76.98 ± 3.59
			Sensitivity	73.26 ± 10.44	-	67.87 ± 3.73	68.44 ± 7.06	75.43 ± 9.65	77.83 ± 4.00
			Specificity	68.54 ± 4.04	-	56.73 ± 4.10	54.21 ± 7.81	63.34 ± 9.40	76.20 ± 4.27
		RF	Accuracy	65.29 ± 10.17	-	58.23 ± 10.90	62.94 ± 10.02	65.88 ± 10.67	77.06 ± 10.91 ↑
			Sensitivity	66.47 ± 16.13	-	56.64 ± 16.22	63.90 ± 22.11	62.13 ± 19.44	80.91 ± 16.46
			Specificity	64.78 ± 16.34	-	61.65 ± 17.19	62.36 ± 16.67	70.86 ± 10.31	73.83 ± 19.36
		SVM	Accuracy	57.47 ± 3.03	-	60.65 ± 1.95	62.66 ± 3.28	65.40 ± 2.21	61.25 ± 8.88
			Sensitivity	44.22 ± 3.85	-	52.24 ± 3.88	54.58 ± 3.29	61.08 ± 5.28	53.71 ± 10.61
			Specificity	70.73 ± 7.30	-	68.86 ± 4.10	70.64 ± 9.16	69.74 ± 4.34	68.77 ± 16.22
Males	Linear	KNN	Accuracy	-	80.26 ± 3.36	74.14 ± 5.02	71.64 ± 6.98	95.50 ± 1.95 ↑	83.77 ± 3.17
			Sensitivity	-	84.66 ± 4.22	76.31 ± 4.28	72.90 ± 5.45	95.30 ± 2.11	88.48 ± 6.23
			Specificity	-	75.66 ± 3.37	71.88 ± 6.38	70.40 ± 11.57	95.71 ± 2.65	79.33 ± 2.36
		LDA	Accuracy	-	71.72 ± 2.87	73.02 ± 6.00	79.95 ± 5.20	84.65 ± 1.42	81.34 ± 1.64
			Sensitivity	-	86.22 ± 1.74	86.97 ± 3.32	84.66 ± 4.92	92.12 ± 2.47	94.03 ± 2.31
			Specificity	-	57.22 ± 5.72	58.59 ± 9.92	75.22 ± 6.28	77.21 ± 3.83	68.18 ± 4.79
		RF	Accuracy	-	75.33 ± 9.45	75.33 ± 11.35	72.00 ± 10.79	92.00 ± 6.88	94.67 ± 5.26
			Sensitivity	-	72.91 ± 7.26	80.46 ± 13.46	70.40 ± 17.77	90.36 ± 8.89	95.22 ± 7.98
			Specificity	-	77.58 ± 14.83	72.72 ± 14.71	75.13 ± 19.06	94.70 ± 9.65	93.35 ± 7.52
		SVM	Accuracy	-	77.21 ± 2.13	77.81 ± 6.47	77.72 ± 5.20	89.18 ± 5.32	90.98 ± 2.10
			Sensitivity	-	72.88 ± 6.45	76.24 ± 9.56	81.63 ± 4.11	95.63 ± 2.79	87.06 ± 3.71
			Specificity	-	81.27 ± 3.47	79.40 ± 3.98	73.74 ± 6.87	82.71 ± 8.10	94.81 ± 3.45
	Nonlinear	KNN	Accuracy	65.84 ± 3.54	51.19 ± 2.81	62.33 ± 6.60	68.90 ± 3.37	61.52 ± 2.60	60.15 ± 3.61
			Sensitivity	67.44 ± 9.30	55.88 ± 6.38	57.45 ± 3.01	67.03 ± 2.89	60.83 ± 4.63	59.73 ± 7.61
			Specificity	64.24 ± 4.38	46.53 ± 3.17	67.15 ± 12.37	70.87 ± 7.31	62.21 ± 4.16	60.58 ± 11.01
		LDA	Accuracy	68.17 ± 7.09	58.96 ± 2.47	65.14 ± 5.01	66.98 ± 4.55	61.95 ± 3.25	74.26 ± 6.46
			Sensitivity	64.73 ± 13.46	64.20 ± 5.20	64.92 ± 7.04	73.63 ± 5.34	61.20 ± 3.35	79.21 ± 7.42
			Specificity	71.67 ± 3.28	53.60 ± 4.42	65.36 ± 5.76	60.35 ± 14.01	62.70 ± 3.87	69.32 ± 7.24
		RF	Accuracy	62.67 ± 14.81	55.33 ± 9.45	67.33 ± 10.16	80.67 ± 10.63	68.67 ± 12.59	82.67 ± 8.43 ↑
			Sensitivity	71.59 ± 15.17	54.47 ± 13.30	67.46 ± 16.35	75.97 ± 17.68	60.35 ± 18.44	83.01 ± 12.58
			Specificity	49.90 ± 24.90	57.43 ± 13.30	68.08 ± 17.55	86.99 ± 12.12	81.85 ± 15.66	84.18 ± 13.72
		SVM	Accuracy	71.79 ± 6.01	56.33 ± 2.80	68.11 ± 2.81	79.21 ± 2.57	72.89 ± 7.69	68.40 ± 6.34
			Sensitivity	73.87 ± 9.89	67.85 ± 5.12	78.29 ± 3.78	75.60 ± 3.33	69.46 ± 12.28	87.93 ± 3.54
			Specificity	69.72 ± 4.09	44.84 ± 5.68	56.27 ± 4.97	82.82 ± 4.65	76.48 ± 6.49	48.88 ± 13.38
All Subjects	Linear	KNN	Accuracy	59.98 ± 2.64	68.18 ± 2.78	65.53 ± 4.10	72.09 ± 2.97	81.99 ± 1.78	80.71 ± 0.80
			Sensitivity	62.48 ± 6.90	64.64 ± 4.67	68.81 ± 3.75	76.36 ± 4.54	83.33 ± 1.80	80.98 ± 1.34
			Specificity	57.52 ± 2.53	71.73 ± 8.18	62.21 ± 4.56	67.65 ± 2.68	80.67 ± 2.84	80.45 ± 1.44
		LDA	Accuracy	64.16 ± 5.02	67.12 ± 3.07	65.69 ± 1.97	68.81 ± 2.34	65.15 ± 1.77	72.64 ± 2.46
			Sensitivity	74.56 ± 4.13	75.51 ± 5.13	72.68 ± 2.37	84.31 ± 6.62	71.04 ± 3.68	70.05 ± 4.78
			Specificity	53.57 ± 6.57	58.76 ± 3.33	58.72 ± 3.08	53.13 ± 3.99	59.31 ± 5.34	75.31 ± 6.72
		RF	Accuracy	61.93 ± 9.83	75.16 ± 5.90	67.42 ± 11.92	80.32 ± 8.25	82.90 ± 5.49	90.32 ± 6.80 ↑
			Sensitivity	65.93 ± 17.89	74.59 ± 8.15	65.31 ± 14.08	79.65 ± 13.61	80.97 ± 10.25	92.66 ± 7.81
			Specificity	57.11 ± 10.94	74.73 ± 8.51	69.81 ± 12.05	80.90 ± 5.96	85.70 ± 9.72	88.92 ± 10.56
		SVM	Accuracy	60.74 ± 3.83	68.23 ± 2.59	68.58 ± 2.52	73.14 ± 2.16	80.10 ± 2.61	85.62 ± 1.81
			Sensitivity	61.36 ± 5.74	76.57 ± 4.09	74.30 ± 1.93	80.98 ± 4.95	81.61 ± 2.52	76.37 ± 5.41
			Specificity	60.07 ± 3.71	59.94 ± 4.56	62.77 ± 5.17	65.22 ± 1.97	78.60 ± 3.53	94.90 ± 3.24
	Nonlinear	KNN	Accuracy	58.65 ± 1.33	54.12 ± 4.01	56.65 ± 2.67	58.90 ± 5.66	67.30 ± 3.25	71.10 ± 4.74
			Sensitivity	57.42 ± 1.53	53.07 ± 5.70	52.77 ± 7.64	56.96 ± 9.57	71.97 ± 4.19	67.27 ± 6.37
			Specificity	59.88 ± 2.17	55.17 ± 2.74	60.54 ± 3.44	60.81 ± 5.49	62.60 ± 3.12	74.91 ± 3.97
		LDA	Accuracy	59.96 ± 2.30	56.44 ± 4.34	58.89 ± 1.38	62.95 ± 7.64	69.31 ± 5.49	69.14 ± 4.32
			Sensitivity	59.89 ± 3.26	60.96 ± 6.48	58.03 ± 2.72	62.84 ± 4.49	75.03 ± 9.67	65.56 ± 4.68
			Specificity	60.09 ± 5.13	51.82 ± 3.34	59.72 ± 2.20	63.05 ± 11.51	63.79 ± 2.97	72.69 ± 4.19
		RF	Accuracy	60.00 ± 4.08	50.97 ± 3.33	63.22 ± 6.49	62.58 ± 5.93	68.71 ± 10.86	73.55 ± 9.10 ↑
			Sensitivity	56.90 ± 8.92	48.59 ± 8.90	58.97 ± 14.89	63.18 ± 7.69	65.92 ± 15.90	73.19 ± 11.17
			Specificity	63.72 ± 9.75	53.23 ± 12.57	67.97 ± 12.65	62.24 ± 9.43	71.75 ± 9.13	73.07 ± 11.09
		SVM	Accuracy	61.24 ± 4.37	53.48 ± 1.72	65.27 ± 3.60	61.80 ± 1.43	66.76 ± 2.97	68.40 ± 3.41
			Sensitivity	43.91 ± 3.06	51.26 ± 7.88	58.86 ± 5.35	56.84 ± 1.79	69.64 ± 4.40	82.52 ± 2.40
			Specificity	78.44 ± 8.00	55.52 ± 6.56	71.80 ± 5.40	66.87 ± 2.98	63.84 ± 3.91	54.45 ± 7.71

TABLE 5. Classification results for dislike task in CL/BW images using linear and nonlinear features, across different groups.

1-10 Group	Features	Classifier	Metric	Delta	Theta	Alpha	Beta	Gamma	All Bands
Females	Linear	KNN	Accuracy	78.71 ± 3.56	94.14 ± 3.30	73.99 ± 1.71	90.82 ± 4.50	72.64 ± 5.37	87.02 ± 3.23
			Sensitivity	72.99 ± 4.94	93.98 ± 4.31	78.55 ± 4.58	91.33 ± 4.95	74.44 ± 2.97	90.49 ± 6.22
			Specificity	84.15 ± 4.30	94.31 ± 2.67	69.47 ± 4.18	90.34 ± 4.67	70.86 ± 10.35	83.88 ± 2.56
		LDA	Accuracy	83.74 ± 2.69	79.02 ± 3.15	69.26 ± 7.43	76.36 ± 3.91	85.11 ± 5.98	89.71 ± 2.64
			Sensitivity	82.66 ± 3.38	95.57 ± 1.99	72.61 ± 8.46	67.79 ± 6.76	90.36 ± 3.93	88.41 ± 3.30
			Specificity	84.81 ± 4.94	62.48 ± 5.00	65.77 ± 7.97	84.67 ± 10.49	79.89 ± 8.53	91.03 ± 3.86
		RF	Accuracy	90.62 ± 5.31	93.12 ± 4.61	73.12 ± 13.83	91.25 ± 7.34	95.62 ± 4.22	96.87 ± 3.29 ↑
			Sensitivity	91.23 ± 7.97	94.68 ± 7.04	78.84 ± 18.50	93.30 ± 10.76	96.87 ± 5.17	97, 64 ± 4.99
			Specificity	90.09 ± 7.73	92.61 ± 5.34	65.99 ± 18.13	91.01 ± 8.26	95.75 ± 7.27	94.72 ± 9.11
		SVM	Accuracy	84.56 ± 6.74	88.86 ± 2.68	74.04 ± 5.90	82.51 ± 4.30	90.03 ± 2.22	91.22 ± 2.42
			Sensitivity	86.56 ± 8.75	85.45 ± 1.51	79.12 ± 4.16	83.68 ± 7.42	93.23 ± 2.32	91.43 ± 3.46
			Specificity	82.68 ± 5.21	92.07 ± 5.02	69.16 ± 9.67	81.14 ± 2.41	86.84 ± 5.77	91.04 ± 4.19
	Nonlinear	KNN	Accuracy	59.92 ± 6.02	53.14 ± 4.56	57.29 ± 3.10	80.78 ± 5.03	65.96 ± 2.03	85.91 ± 7.25 ↑
			Sensitivity	60.11 ± 2.17	46.22 ± 6.95	61.90 ± 6.28	81.13 ± 6.94	75.76 ± 4.92	88.69 ± 8.68
			Specificity	59.68 ± 11.10	59.89 ± 5.10	52.73 ± 5.12	80.49 ± 4.07	55.57 ± 6.09	83.01 ± 6.83
		LDA	Accuracy	63.93 ± 7.50	65.54 ± 3.66	63.72 ± 3.76	80.96 ± 4.91	51.73 ± 2.43	81.97 ± 6.47
			Sensitivity	62.01 ± 5.76	66.25 ± 5.09	53.01 ± 7.32	85.34 ± 7.09	26.23 ± 5.34	85.49 ± 5.12
			Specificity	66.09 ± 10.47	64.83 ± 4.46	74.21 ± 4.18	76.56 ± 3.96	25.17 ± 6.81	78.49 ± 9.24
		RF	Accuracy	61.25 ± 9.68	53.12 ± 7.93	59.37 ± 10.72	80.62 ± 9.06	70.62 ± 14.14	81.25 ± 12.50
			Sensitivity	66.93 ± 15.70	51.33 ± 15.35	60.17 ± 16.12	82.10 ± 18.60	73.09 ± 21.87	89.31 ± 15.78
			Specificity	51.00 ± 20.53	55.09 ± 16.46	60.78 ± 19.34	76.40 ± 13.39	70.22 ± 18.56	75.74 ± 14.60
		SVM	Accuracy	63.74 ± 2.80	67.95 ± 6.33	63.38 ± 3.99	85.52 ± 3.92	71.23 ± 7.21	66.30 ± 5.99
			Sensitivity	62.98 ± 5.19	69.61 ± 5.89	73.95 ± 3.08	89.60 ± 3.09	85.56 ± 7.97	8.79 ± 7.47
			Specificity	64.50 ± 2.37	66.32 ± 11.03	53.12 ± 7.59	81.39 ± 3.36	56.38 ± 7.33	53.74 ± 10.23
Males	Linear	KNN	Accuracy	-	83.21 ± 4.69	74.46 ± 2.05	74.91 ± 7.19	90.88 ± 4.14	91.84 ± 1.10
			Sensitivity	-	80.56 ± 8.52	71.56 ± 5.27	74.56 ± 9.99	92.39 ± 4.06	91.05 ± 2.71
			Specificity	-	85.86 ± 2.15	77.36 ± 8.30	75.17 ± 4.67	89.41 ± 4.54	92.63 ± 3.01
		LDA	Accuracy	-	65.01 ± 4.96	61.64 ± 4.61	66.06 ± 5.60	76.27 ± 4.65	71.47 ± 3.86
			Sensitivity	-	72.63 ± 4.05	69.14 ± 4.35	80.80 ± 5.03	83.09 ± 4.10	82.86 ± 2.36
			Specificity	-	57.43 ± 5.28	53.92 ± 5.58	50.35 ± 7.94	69.67 ± 12.57	59.69 ± 6.86
		RF	Accuracy	-	81.33 ± 9.84	80.00 ± 14.40	69.33 ± 4.66	90.00 ± 7.20	96.67 ± 3.51 ↑
			Sensitivity	-	85.84 ± 15.71	80.03 ± 21.15	74.09 ± 15.02	89.74 ± 9.03	96.32 ± 6.01
			Specificity	-	76.19 ± 16.84	81.37 ± 14.89	69.71 ± 14.76	91.21 ± 7.84	97.75 ± 4.78
		SVM	Accuracy	-	80.09 ± 4.65	76.08 ± 9.61	68.83 ± 4.28	90.55 ± 4.48	88.12 ± 2.94
			Sensitivity	-	81.61 ± 3.35	74.43 ± 11.03	77.29 ± 3.95	91.22 ± 4.75	80.05 ± 3.51
			Specificity	-	78.54 ± 6.34	77.79 ± 8.88	60.64 ± 6.48	89.87 ± 4.50	95.94 ± 2.51
	Nonlinear	KNN	Accuracy	-	67.20 ± 6.65	61.44 ± 4.23	70.89 ± 3.83	61.57 ± 4.63	65.59 ± 5.31
			Sensitivity	-	61.97 ± 3.15	57.17 ± 4.61	74.24 ± 9.73	64.40 ± 5.68	76.06 ± 9.21
			Specificity	-	72.05 ± 12.71	65.87 ± 6.00	67.89 ± 3.14	58.66 ± 7.12	55.11 ± 3.81
		LDA	Accuracy	-	52.07 ± 2.91	48.27 ± 3.40	54.28 ± 2.3	50.25 ± 2.41	70.63 ± 3.69
			Sensitivity	-	21.89 ± 4.46	25.42 ± 3.93	19.78 ± 5.00	23.61 ± 4.93	73.21 ± 9.62
			Specificity	-	46.27 ± 3.23	36.17 ± 5.67	23.06 ± 3.42	31.24 ± 3.81	67.75 ± 5.14
		RF	Accuracy	-	66.67 ± 7.03	53.33 ± 12.17	76.67 ± 9.03	74.00 ± 13.50	84.00 ± 7.17 ↑
			Sensitivity	-	54.48 ± 23.68	55.58 ± 17.10	78.15 ± 14.11	77.08 ± 12.62	84.25 ± 7.24
			Specificity	-	77.32 ± 14.25	53.15 ± 15.07	74.07 ± 16.14	70.13 ± 19.11	83.87 ± 7.77
		SVM	Accuracy	-	70.55 ± 5.23	66.07 ± 6.73	82.41 ± 8.24	62.78 ± 4.27	63.95 ± 3.54
			Sensitivity	-	77.01 ± 6.28	58.59 ± 6.36	75.85 ± 12.20	79.25 ± 12.46	79.10 ± 9.90
			Specificity	-	64.40 ± 5.94	73.53 ± 8.95	88.91 ± 4.93	46.20 ± 7.28	48.81 ± 10.72
All Subjects	Linear	KNN	Accuracy	69.68 ± 3.33	85.50 ± 4.34	66.59 ± 2.95	76.70 ± 3.27	74.25 ± 3.61	86.35 ± 2.57
			Sensitivity	75.28 ± 5.46	87.66 ± 2.93	71.88 ± 4.84	73.10 ± 1.59	74.13 ± 7.29	88.80 ± 4.61
			Specificity	64.15 ± 2.28	83.34 ± 6.43	61.30 ± 2.23	80.35 ± 7.18	74.43 ± 1.87	83.91 ± 2.23
		LDA	Accuracy	66.14 ± 1.53	76.86 ± 5.04	61.00 ± 1.85	65.77 ± 2.05	67.25 ± 2.25	76.41 ± 1.54
			Sensitivity	73.82 ± 3.35	83.86 ± 3.77	69.50 ± 1.77	71.17 ± 2.86	73.99 ± 3.38	83.00 ± 1.83
			Specificity	58.47 ± 3.62	69.90 ± 7.46	52.48 ± 2.42	60.50 ± 5.70	60.52 ± 2.21	69.74 ± 2.03
		RF	Accuracy	70.00 ± 3.85	81.00 ± 5.45	69.00 ± 10.31	72.00 ± 9.45	92.33 ± 3.86	93.33 ± 2.72 ↑
			Sensitivity	69.47 ± 10.79	81.25 ± 8.53	79.98 ± 13.29	71.73 ± 13.37	93.18 ± 5.64	93.99 ± 4.02
			Specificity	70.09 ± 12.56	79.06 ± 10.74	59.32 ± 16.50	71.04 ± 14.96	91.91 ± 6.31	92.74 ± 5.80
		SVM	Accuracy	70.49 ± 1.97	77.04 ± 2.72	71.36 ± 4.64	66.85 ± 4.93	90.20 ± 1.46	89.51 ± 2.58
			Sensitivity	68.82 ± 2.81	83.90 ± 6.75	85.95 ± 6.00	67.29 ± 4.07	85.02 ± 3.33	83.19 ± 5.52
			Specificity	72.16 ± 2.87	70.18 ± 2.35	56.77 ± 4.72	66.42 ± 7.24	95.37 ± 3.37	95.83 ± 1.09
	Nonlinear	KNN	Accuracy	-	57.70 ± 6.93	59.02 ± 0.88	61.18 ± 1.91	60.61 ± 5.87	63.08 ± 2.47
			Sensitivity	-	59.23 ± 13.14	63.58 ± 2.14	61.28 ± 1.20	58.82 ± 5.75	65.26 ± 4.38
			Specificity	-	56.15 ± 3.80	54.39 ± 1.59	61.08 ± 4.19	62.40 ± 8.37	60.91 ± 2.65
		LDA	Accuracy	-	53.62 ± 3.23	54.52 ± 5.59	62.09 ± 2.92	63.68 ± 1.39	75.93 ± 4.36 ↑
			Sensitivity	-	65.10 ± 3.46	47.52 ± 5.60	66.61 ± 3.31	64.07 ± 2.90	75.28 ± 4.19
			Specificity	-	42.16 ± 4.75	61.54 ± 7.38	57.58 ± 2.72	63.31 ± 2.46	76.57 ± 5.19
		RF	Accuracy	-	56.00 ± 5.40	61.33 ± 8.78	73.33 ± 8.61	64.33 ± 9.69	74.33 ± 6.86
			Sensitivity	-	60.05 ± 13.58	64.28 ± 16.04	75.77 ± 12.00	67.14 ± 17.13	75.90 ± 14.12
			Specificity	-	53.11 ± 9.18	60.96 ± 15.18	71.74 ± 12.30	63.00 ± 10.25	72.63 ± 9.22
		SVM	Accuracy	-	57.03 ± 2.90	66.27 ± 2.63	70.69 ± 1.66	68.08 ± 4.73	68.90 ± 5.53
			Sensitivity	-	60.20 ± 2.40	67.87 ± 6.94	70.53 ± 3.97	75.59 ± 3.88	92.04 ± 5.82
			Specificity	-	53.91 ± 5.44	64.66 ± 2.49	70.82 ± 3.15	60.57 ± 10.76	45.90 ± 8.07

LDA, and SVM. Among the extracted features in the algorithm, both PSD and EDWTC were identified as the most informative. Regarding male subjects, the highest accuracy was achieved using linear features in the Gamma band, with the PSD being the most informative extracted feature in the algorithm. The KNN classifier demonstrated superior performance compared to the other classifiers. For all subjects (females and males), the most effective set of frequency bands in accurately classifying subjects who liked CL/BW stimuli was found to be delta, theta, alpha, beta, and gamma, with a classification accuracy rate of 90.32%, surpassing other feature sets, including nonlinear features. The most informative extracted features were PSD and EDWTC. Moreover, the RF classifier demonstrated superior performance when compared to other classifiers.

Table 5 presents the results of classifying participants who expressed dislike towards CL/BW stimuli using both linear and nonlinear features for different groups. The findings reveal that for female subjects, the most accurate feature set comprises the delta, theta, alpha, beta, and gamma frequency bands. This set achieved a classification accuracy of 96.87%, surpassing other feature sets that included nonlinear features. Moreover, the RF classifier exhibited superior performance compared to other classifiers. Similarly, the combination of theta, alpha, beta, and gamma frequency bands with linear features resulted in the best accuracy of 96.67% for male subjects. The RF classifier outperformed other classifiers in this regard. Moreover, for all subjects, regardless of gender, the delta, theta, alpha, beta, and gamma frequency bands were identified as the most effective feature set for accurately classifying those who disliked CL/BW stimuli. This particular feature set achieved a classification accuracy rate of 93.33%, outperforming other feature sets that included nonlinear features. Additionally, the RF classifier demonstrated superior performance when compared to other classifiers.

Overall, the study indicates that there are significant gender differences in the time taken to make Like and Dislike decisions when viewing CL/BW images. Specifically, females took around 2.5 seconds to decide on both types of images, while males took approximately 2.5 seconds for color images and close to 3 seconds for black-white images, which is consistent with previous research conducted by Whitchalls. Additionally, the decision-making time for Like and Dislike was similar for all groups when viewing black-white images. However, when viewing color images, the Dislike decision took slightly longer than the Like decision, with a mean time of 2.6 ± 0.02 seconds for Dislike and 2.2 ± 0.003 seconds for Like.

IV. CONCLUSION

This study provides new insights into the impact of CL/BW images on preferences and decision-making, as well as their implications for marketing products and neuromarketing strategies. The results demonstrate that different brain regions are activated depending on the subjects' preferences and the color of stimuli. Additionally, the use of non-linear features outperformed linear features in distinguishing channels in men's Like/Dislike tasks. Furthermore, the study identified differences in decision-making times between males and females and between Like and Dislike decisions for color images. The findings suggest that careful selection of stimuli and classifiers is critical for similar classification tasks. This result is interesting and confirms the results reported in [39], where compared with other brain regions, the features of frontal and occipital brain region obtained a higher prediction accuracy. This study has some shortcomings that must be acknowledged. Only product images were used as marketing stimuli with respect to color and gender, and other factors such as brand, ratings, and price were not considered in the experiment. In other words, we concealed those factors (brand, price, etc) to investigate the color and gender factors in the Like/Dislike task. Overall, the study's results have important implications for the field of neuromarketing and highlight the potential benefits of utilizing EEG signals to analyze the impact of CL/BW images on consumer behavior.

REFERENCES

[1] A. Rakshit and R. Lahiri, "Discriminating different color from EEG signals using interval-type 2 fuzzy space classifier (a neuro-marketing study on the effect of color to cognitive state)," in *Proc. IEEE 1st Int. Conf. Power Electron., Intell. Control Energy Syst. (ICPEICES)*, Jul. 2016, pp. 1–6.

[2] M. H. Yun, S. H. Han, S. W. Hong, and J. Kim, "Incorporating user satisfaction into the look-and-feel of mobile phone design," *Ergonomics*, vol. 46, nos. 13–14, pp. 1423–1440, Oct. 2003.

[3] S.-W. Hsiao, "A systematic method for color planning in product design," *Color Res. Appl.*, vol. 20, no. 3, pp. 191–205, Jun. 1995.

[4] S.-W. Hsiao and H.-C. Tsai, "Use of gray system theory in product-color planning," *Color Res. Appl.*, vol. 29, no. 3, pp. 222–231, 2004.

[5] P. Kotler, "Atmospherics as a marketing tool," *J. Retailing*, vol. 49, no. 4, pp. 48–64, 1973.

[6] M.-Y. Ma, C.-Y. Chen, and F.-G. Wu, "A design decision-making support model for customized product color combination," *Comput. Ind.*, vol. 58, no. 6, pp. 504–518, Aug. 2007.

[7] R. S. Cimbalo, K. L. Beck, and D. S. Sendziak, "Emotionally toned pictures and color selection for children and college students," *J. Genet. Psychol.*, vol. 133, no. 2, pp. 303–304, Dec. 1978.

[8] M. Kawasaki and Y. Yamaguchi, "Effects of subjective preference of colors on attention-related occipital theta oscillations," *NeuroImage*, vol. 59, no. 1, pp. 808–814, Jan. 2012.

[9] R. Bagchi and A. Cheema, "The effect of red background color on willingness-to-pay: The moderating role of selling mechanism," *J. Consum. Res.*, vol. 39, no. 5, pp. 947–960, Feb. 2013.

[10] C. S. R. Chan and H. D. Park, "How images and color in business plans influence venture investment screening decisions," *J. Bus. Venturing*, vol. 30, no. 5, pp. 732–748, Sep. 2015.

[11] I. Membreño, B. Rodríguez, L. González, E. Castillero, and R. Cattafi, "Neuroscience and marketing: Influence of color in the predisposition to buy in users of social networks," Sci. Initiation Mag., Technol. Univ. Panama, Panama, Tech. Rep., 2020, vol. 6, no. 1.

[12] D. Rahmadani, H. Fauzi, R. A. Lubis, and M. Ariyanti, "Study of neuromarketing in consumer behavior due to product logos color changes effect," *J. Comput. Eng., Prog., Appl. Technol.*, vol. 1, no. 2, pp. 41–52, 2022.

[13] R. N. Khushaba, L. Greenacre, S. Kodagoda, J. Louviere, S. Burke, and G. Dissanayake, "Choice modeling and the brain: A study on the electroencephalogram (EEG) of preferences," *Expert Syst. Appl.*, vol. 39, no. 16, pp. 12378–12388, Nov. 2012.

[14] B. Yılmaz, S. Korkmaz, D. B. Arslan, E. Güngör, and M. H. Asyalı, "Like/dislike analysis using EEG: Determination of most discriminative channels and frequencies," *Comput. Methods Programs Biomed.*, vol. 113, no. 2, pp. 705–713, Feb. 2014.

[15] P. Golnar-Nik, S. Farashi, and M.-S. Safari, "The application of EEG power for the prediction and interpretation of consumer decision-making: A neuromarketing study," *Physiol. Behav.*, vol. 207, pp. 90–98, Aug. 2019.

[16] G. Cartocci, M. Caratù, E. Modica, A. G. Maglione, D. Rossi, P. Cherubino, and F. Babiloni, "Electroencephalographic, heart rate, and galvanic skin response assessment for an advertising perception study: Application to antismoking public service announcements," *J. Vis. Exp.*, vol. 1, no. 126, Aug. 2017, Art. no. e55872.

[17] T. Z. Ramsøy, M. Skov, M. K. Christensen, and C. Stahlhut, "Frontal brain asymmetry and willingness to pay," *Frontiers Neurosci.*, vol. 12, p. 138, Mar. 2018.

[18] M. Aldayel, M. Ykhlef, and A. Al-Nafjan, "Deep learning for EEG-based preference classification in neuromarketing," *Appl. Sci.*, vol. 10, no. 4, p. 1525, Feb. 2020.

[19] M. Aldayel, M. Ykhlef, and A. Al-Nafjan, "Recognition of consumer preference by analysis and classification EEG signals," *Frontiers Hum. Neurosci.*, vol. 14, Jan. 2021, Art. no. 604639.

[20] D.-W. Chen, R. Miao, W.-Q. Yang, Y. Liang, H.-H. Chen, L. Huang, C.-J. Deng, and N. Han, "A feature extraction method based on differential entropy and linear discriminant analysis for emotion recognition," *Sensors*, vol. 19, no. 7, p. 1631, Apr. 2019.

[21] V. M. Joshi and R. B. Ghongade, "EEG based emotion investigation from various brain region using deep learning algorithm," in *Proc. 2nd Int. Conf. Data Sci., Mach. Learn. Appl. (ICDSMLA)*. Singapore: Springer, 2022, pp. 395–402.

[22] L. Bell, J. Vogt, C. Willemse, T. Routledge, L. T. Butler, and M. Sakaki, "Beyond self-report: A review of physiological and neuroscientific methods to investigate consumer behavior," *Frontiers Psychol.*, vol. 9, p. 1655, Sep. 2018.

[23] M. Kim and S.-P. Kim, "A comparsion of artifact rejection methods for a BCI using event related potentials," in *Proc. 6th Int. Conf. Brain-Comput. Interface (BCI)*, Jan. 2018, pp. 1–4.

[24] M. Plechawska-Wojcik, M. Kaczorowska, and D. Zapala, "The artifact subspace reconstruction (ASR) for EEG signal correction. A comparative study," in *Proc. Int. Conf. Inf. Syst. Archit. Technol.* Switzerland: Springer, 2018, pp. 125–135.

[25] A. Hekmatmanesh, H. M. Azni, H. Wu, M. Afsharchi, M. Li, and H. Handroos, "Imaginary control of a mobile vehicle using deep learning algorithm: A brain computer interface study," *IEEE Access*, vol. 10, pp. 20043–20052, 2022.

[26] UCSD. (2021). *ICLabel Tutorial: EEG Independent Component Labeling*. Accessed: Jan. 3, 2021. [Online]. Available: https://labeling.ucsd.edu/tutorial/labels

[27] A. Delorme and S. Makeig, "EEGLAB: An open source toolbox for analysis of single-trial EEG dynamics including independent component analysis," *J. Neurosci. Methods*, vol. 134, no. 1, pp. 9–21, Mar. 2004.

[28] A. Hekmatmanesh, H. Wu, and H. Handroos, "Largest Lyapunov exponent optimization for control of a bionic-hand: A brain computer interface study," *Frontiers Rehabil. Sci.*, vol. 2, Feb. 2022, Art. no. 802070.

[29] A. Hassani, A. Hekmatmanesh, and A. M. Nasrabadi, "Discrimination of customers decision-making in a like/dislike shopping activity based on genders: A neuromarketing study," *IEEE Access*, vol. 10, pp. 92454–92466, 2022.

[30] M. Hollander, D. A. Wolfe, and E. Chicken, *Nonparametric Statistical Methods*, vol. 751. Hoboken, NJ, USA: Wiley, 2013.

[31] A. Hekmatmanesh, H. Wu, F. Jamaloo, M. Li, and H. Handroos, "A combination of CSP-based method with soft margin SVM classifier and generalized RBF kernel for imagery-based brain computer interface applications," *Multimedia Tools Appl.*, vol. 79, nos. 25–26, pp. 17521–17549, Jul. 2020.

[32] S. Zhang, "Nearest neighbor selection for iteratively kNN imputation," *J. Syst. Softw.*, vol. 85, no. 11, pp. 2541–2552, Nov. 2012.

[33] T. Wang, Z. Qin, S. Zhang, and C. Zhang, "Cost-sensitive classification with inadequate labeled data," *Inf. Syst.*, vol. 37, no. 5, pp. 508–516, Jul. 2012.

[34] X. Zhu, X. Li, and S. Zhang, "Block-row sparse multiview multilabel learning for image classification," *IEEE Trans. Cybern.*, vol. 46, no. 2, pp. 450–461, Feb. 2016.

[35] K. Zhang, X. Gao, D. Tao, and X. Li, "Single image super-resolution with multiscale similarity learning," *IEEE Trans. Neural Netw. Learn. Syst.*, vol. 24, no. 10, pp. 1648–1659, Oct. 2013.

[36] S. R. Safavian and D. Landgrebe, "A survey of decision tree classifier methodology," *IEEE Trans. Syst., Man, Cybern.*, vol. 21, no. 3, pp. 660–674, 1991.

[37] H. Liu, X. Li, and S. Zhang, "Learning instance correlation functions for multilabel classification," *IEEE Trans. Cybern.*, vol. 47, no. 2, pp. 499–510, Feb. 2017.

[38] A. Hekmatmanesh, H. Wu, M. Li, and H. Handroos, "A combined projection for remote control of a vehicle based on movement imagination: A single trial brain computer interface study," *IEEE Access*, vol. 10, pp. 6165–6174, 2022.

[39] L. Zeng, M. Lin, K. Xiao, J. Wang, and H. Zhou, "Like/dislike prediction for sport shoes with electroencephalography: An application of neuromarketing," *Frontiers Hum. Neurosci.*, vol. 15, Jan. 2022, Art. no. 793952.

ATEFE HASSANI received the B.Sc. degree in electrical engineering from the University of Zanjan, Iran, in 2017, and the M.Sc. degree in biomedical engineering from Shahed University, Tehran, Iran, in 2020. Her current research interests include biomedical signal processing, machine learning, deep learning, and computational neuroscience.

AMIN HEKMATMANESH received the bachelor's degree in electrical engineering from the Science and Research of Fars University, Shiraz, Iran, in 2010, the master's degree in biomedical engineering from Shahed University, Tehran, Iran, in 2013, and the Ph.D. degree in brain-controlled ankle foot and hand orthosis and mobile vehicle robots using the EEG from the Laboratory of Intelligent Machines, Lappeenranta University of Technology, in 2019. His master's thesis was about analyzing sleep EEG signal processing, learning, and negative emotional memory. Since 2020, he has been a Postdoctoral Researcher on heavy machine operator's health monitoring and signal processing for horse simulators with the Laboratory of Intelligent Machines, Lappeenranta University of Technology.

ALI MOTIE NASRABADI received the B.Sc. degree in electronic engineering and the M.Sc. and Ph.D. degrees in biomedical engineering from the Amirkabir University of Technology, Tehran, Iran, in 1994, 1999, and 2004, respectively. In 2004, he joined the Biomedical Engineering Department, Faculty of Engineering, Shahed University, where he was an Assistant Professor, from 2004 to 2011, an Associate Professor, from 2011 to 2017, and he has been a Full Professor, since 2017. He is currently a Scientific Advisor with the National Brain Mapping Laboratory, University of Tehran, Iran. His current research interests include brain–computer interfaces, biomedical signal processing, machine learning, deep learning, nonlinear time series analysis, and computational neuroscience. He is a Board Member of the Iranian Society for Biomedical Engineering and has served on the scientific committees for several national conferences and review boards of five scientific journals.